Journal of Optoelectronic and Biomedical Materials Vol. 16, No. 4, October–December 2024, p. 189-197

Green synthesis of zinc oxide nanoparticles doped Leucas aspera leaf extract and its photocatalytic applications

V. C. Senthilkumar[a,*], N. Bhadusha[a], R. Uthrakumar[b], K. Kaviyarasu[c]
[a]*Department of Chemistry, Govt. Arts College (Autonomous), Salem - 636007, Tamil Nadu, India*
[b]*Department of Physics, Govt. Arts College (Autonomous), Salem - 636007, Tamil Nadu, India*
[c]*UNESCO-UNISA Africa Chair in Nanosciences/Nanotechnology Laboratories, College of Graduate Studies, University of South Africa (UNISA), Muckleneuk Ridge, PO Box 392, Pretoria, South Africa*

Zinc oxide (ZnO) nanoparticles have been produced from the leaf extract of Leucas aspera by utilising a straight forward co-precipitation technique in a green synthesis strategy. The produced nanoparticles are examined by photocatalytic analysis, FTIR, XRD, UV–visible, and SEM. ZnO-related distinctive peaks were visible in the FTIR spectra. The XRD investigation verifies that the produced nanoparticles have a hexagonal crystal structure. Doped ZnO utilising leaf extract has surface morphology that is practically spherical in shape and has minimal aggregation, according to SEM analysis. ZnO-LA composite's photocatalytic dye degradation effectiveness against visible light irradiations is approximately 83%.

(Received July 16, 2024; Accepted October 22, 2024)

Keywords: ZnO nanoparticles, Organic dye, UV-Visible, Photocatalytic performance, Transmission electron microscopy, Advanced oxidation process

1. Introduction

Numerous technological and industrial fields, including environmental science, food technology, biotechnology, health, information science, energy, transportation, and so on, are being modernised in large part thanks to nanotechnology. Because nanotechnology can modify a material's properties at incredibly small sizes, it has had a tremendous impact on the development of materials science research. The majority of nanoparticles are created using bottom-up techniques like hydrothermal, spray pyrolysis, chemical vapour deposition, and sol-gel procedures, as well as top-down techniques like sputtering, lithography, and ball milling. The size and structure of the nanoparticles can be manipulated by adjusting the chemical concentrations and reaction conditions, particularly in chemical procedures. However, these techniques are costly, dangerous, and poisonous, and often produce unintended byproducts.

Green synthesis techniques are getting a lot of interest as a solution to these problems because of its affordability, environmental friendliness, and biocompatibility. Zinc oxide (ZnO) is one of the many metal oxides that has generated a lot of attention in the industrial and commercial domains due to its numerous uses and distinct characteristics. Using a green synthesis technique, ZnO nanoparticles are created from a variety of biological sources, including plant, fruit, fungus, algae, and bacterial extracts. A quick and easy way to create nanoparticles on a wide scale is through green synthesis, which uses extracts from plants. The plant extract increases the material's surface area, which helps it function as a reducing agent to lower the particle size. Leucas aspera fresh leaves are used in traditional medicine and contain a variety of medicinal ingredients. The current work investigates the structural, optical, and photocatalytic properties of ZnO doped Leucas aspera leaf extract nanoparticles that are created utilising a straightforward co-precipitation approach with Leucas aspera leaf extract serving as a capping and stabilising agent.

* Corresponding author: vcschem78@gmail.com
https://doi.org/10.15251/JOBM.2024.164.189

2. Experimental methods

The most popular, straightforward, and affordable approach for creating ZnO doped LA nanoparticles is co-precipitation. In order to create ZnO nanoparticles, 50 millilitres of deionized water and 0.35 millimetres of zinc acetate dehydrate are combined, and the mixture is constantly agitated at 85 degrees Celsius for two hours. To get rid of the contaminants, the precipitated particles are cleaned twice or three times using ethanol. The resulting powder particles are stored for a day at 100° C in a hot air oven and for two hours at 400° C in a muffle furnace. ZnO doped LA nanoparticles are created by adding 10 ml of Leucas aspera leaf extract, 0.35 M of zinc acetate dihydrate, and 50 ml of distilled water. The mixture is then agitated for one hour. The pH of the solution is maintained at 13 by adding sodium hydroxide pellets. Then the similar drying procedure used for ZnO is followed to obtain ZnO LA nanoparticles the experimental procedure is shown in figure 1.

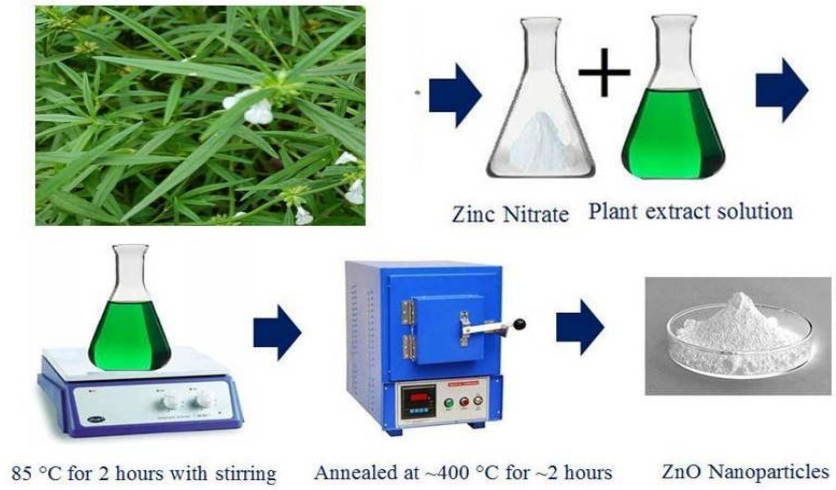

Fig. 1. Biosynthesis of ZnO Leucas aspera leaf extract.

3. Results and discussion

3.1. X-RAY diffraction analysis

The XRD pattern of undoped ZnO NPs is displayed by X-ray diffraction, a non-destructive analytical method that provides comprehensive information about the chemical composition and crystallographic structures of natural and manmade materials. The XRD pattern's prominent diffraction peaks indicate that the sample is crystalline. According to the standard JCPDS data card, the hexagonal wurtzite crystal structure of ZnO is represented by the standard diffraction peaks (JCPDS Card No: 00–001-1136). The absence of any impurity diffraction peaks demonstrated the unadulterated ZnO's purity. Using the Debye-Scherer formula, the average grain size of the un-doped ZnO NPs was determined from the three most intense peaks. Un-doped ZnO NPs had an average grain size of 43.72 nm as a result. Fig. 2 displays the typical XRD patterns of doped ZnO NPs made using leaf extract. Additional peaks corresponding to phases and impurities associated to zinc were observed in the XRD pattern. The XRD spectrum likewise displayed the same peak pattern as the doped ZnO NPs XRD spectrum. The sample synthesised by procedure 2 had an average grain size of 43 nm, which was determined by utilising Debye-Scherer's technique to calculate the three most intense peaks.

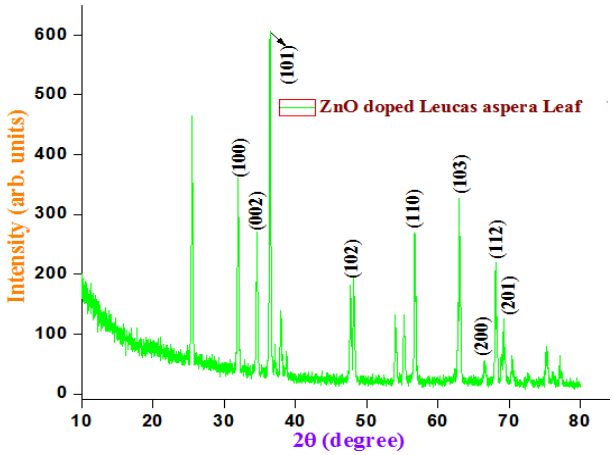

Fig.2. Powder X-ray diffraction pattern of LA doped ZnO NPs samples.

3.2. UV–Vis analysis

The UV–vis absorbance of ZnO NPs doped with synthetic LA was measured between 200 and 1200 nm in wavelength. Figure 3 illustrates how the successful production of doped ZnO NPs is indicated by the existence of distinct peaks in the UV–vis spectra at 388 nm. The prepared doped ZnO NPs with a doping concentration of 10 ML leaf extract were compared, and it was found that the latter's absorption edge was marginally pushed towards lower energy. A decrease in the band gap may be the cause of this change in the absorption edge, according to a prior report. Based on optical absorption spectra, the energy band gap values are calculated using the Tauc relationship (equ. 1).

$$\alpha h\nu = A(h\nu - Eg)n \alpha h\nu = A(h\nu - Eg)n \quad (1)$$

where n is an index that describes the optical absorption, α is the absorption coefficient, h is the plank's constant, v is the photon frequency, A is a constant, and Eg is the band gap. For pure LA-doped ZnO NPs, the predicted band gap energies are 3.25, respectively. When LA leaf extract is added to ZnO crystals, the band gap energy decreases and the absorption band widens, increasing the crystals' ability to absorb light. Conflicting results about the impact of doping ZnO NPs with LA leaf extract on the band gap have been reported in earlier studies. Several factors, such as particle size, oxygen deprivation, and doped ZnO NPs, can be responsible for the observed disparity in the less absorption in the visible area, surface roughness, and lattice strain.

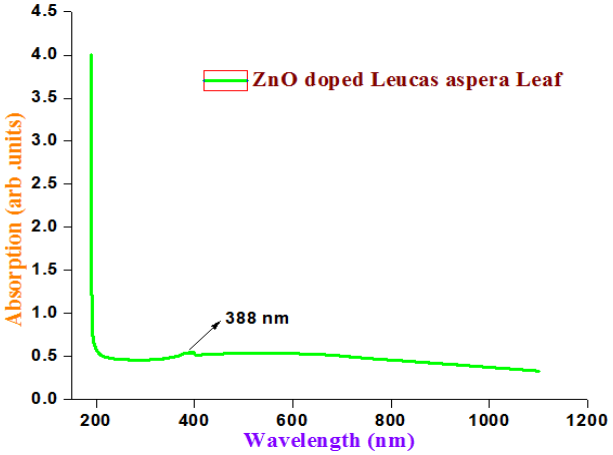

Fig.3. UV-Vis DRS spectra of LA doped ZnO NPs.

3.3. FT-IR spectral studies

In order to ascertain if biological activities were attributed to synthesised LA leaf extract doped ZnO nanoparticles or to biomolecules of plant extracts that might be embedded in the nanoparticle surfaces, FTIR findings were obtained at room temperature and within the 400 cm^{-1} to 4000 cm^{-1} range. Because interatomic vibrations cause absorption bands to typically appear in the fingerprint area of metal oxides. Figure 4 illustrates the hexagonal ZnO wurtzite structure formed by the unusual Zinc oxide absorption band with stretching mode of ZnO, as revealed by IR spectra in the current work. This band was found to be between 500 and 590 cm^{-1}. The asymmetric and symmetric stretching H-O-H vibration is the fundamental mode of vibration near 3492.95 cm^{-1}, and it is caused by bending H-O-H vibration bands of chemisorbed water. The 3000–3650 cm^{-1} bands are due to the reversible dissociative absorption of hydrogen on Zn as well as O site [36]. There were no characteristic peaks in the IR spectra's of synthesized NPs that indicate the presence of biomolecules and Leucas aspera plant extracts in the synthesized ZnO nanoparticles through chemisorbed. As in the IR spectra of plant extracts, we can see that there are characteristics peaks of biomolecules at 871 cm^{-1} (C-H), Hence, biological activities were only exhibited by the synthesized nanoparticles and plant extract's biomolecules were not involved.

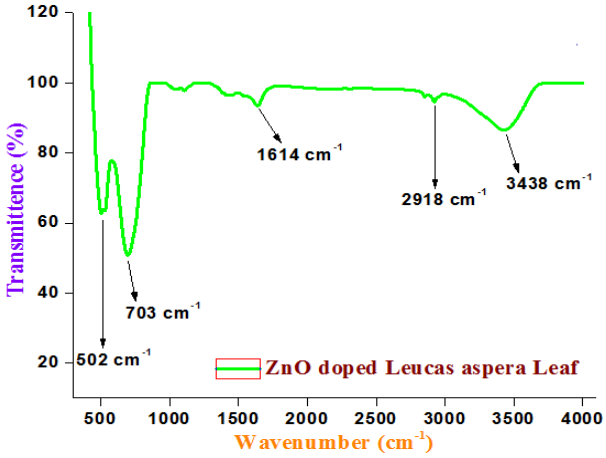

Fig.4. FTIR spectrum of LA doped ZnO NPs samples.

3.4. Surface morphology and composition analysis

SEM examination is utilised to examine the morphological structures of the synthesised nanoparticles. The SEM pictures of LA leaf extract ZnO nanoparticles are displayed in Fig. 5. The low magnification photos made it evident that there hasn't been a complete separation of the particles and that they are agglomerated. Weak physical forces are detected to hold the particles together at greater magnifications. Low magnification SEM pictures of the ZnO nanoparticles are shown in Fig. 5(a–d). When compared to pure ZnO, it is evident that the particles have completely separated and are not as agglomerated.The SEM pictures (Figs. 5c and d) obtained at higher magnification demonstrate that the morphological structure of ZnO nanoparticles doped with LA is nearly spherical. Fig. 5e displays the elemental composition of the nanoparticles that were studied using an EDX spectrum. The production of impurity-free LA-ZnO nanoparticles is confirmed by the EDX spectrums of the two samples: the pure ZnO sample proves the presence of only zinc and oxygen, while the LA-ZnO sample reveals the presence of carbon, zinc, and oxygen.

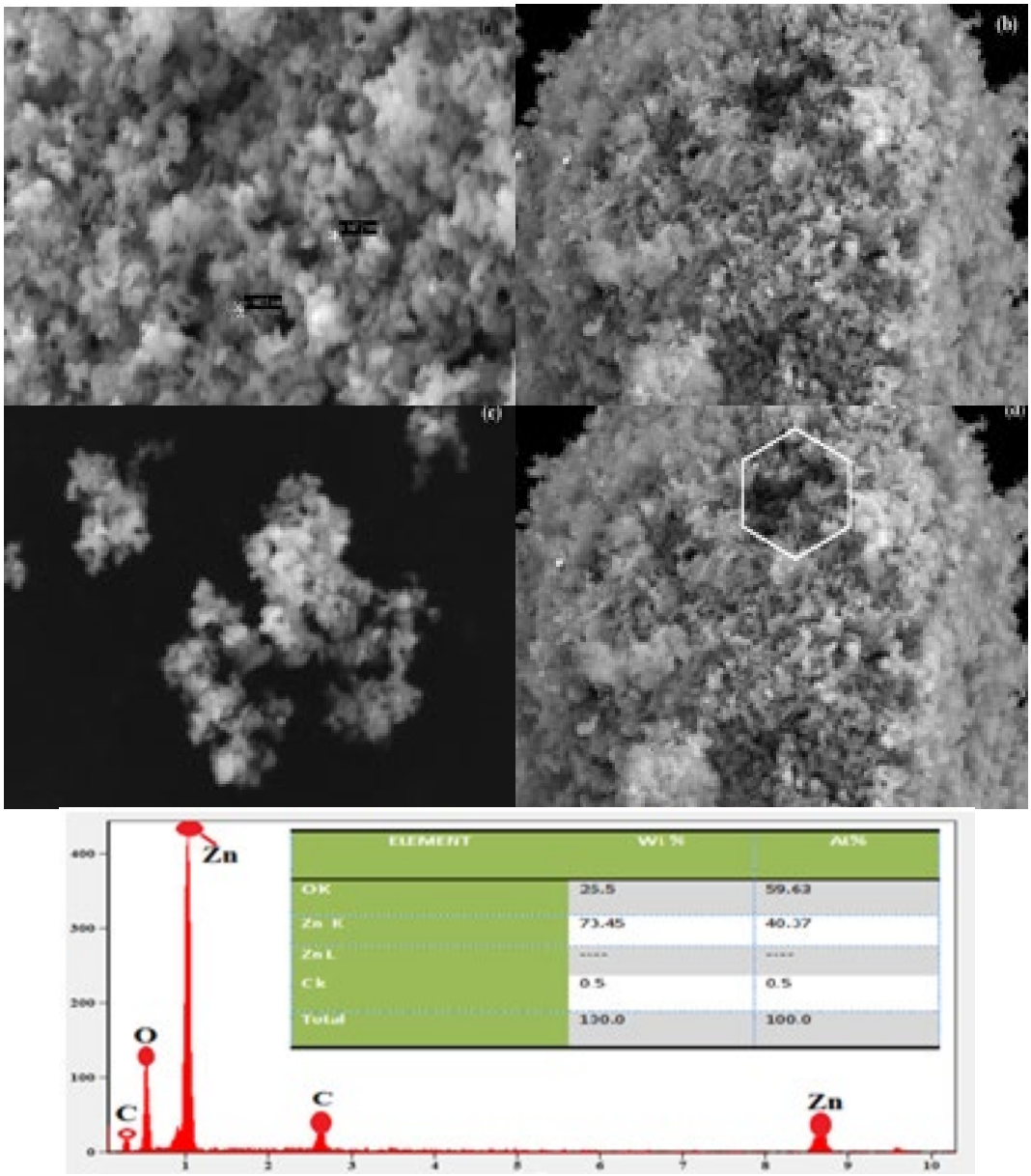

Fig. 5. (a-c) SEM images of LA doped ZnO and (d) EDAX spectra of LA@ZnO NPs.

3.5. Photocatalytic studies

ZnO and leaf extract doped ZnO nanoparticles were tested for their capacity to break down the methylene blue (MB) dye when exposed to sunshine. When the irradiation period increases, the dye solution's colour gradually changes from blue to colourless, and the amount of MB dye absorbed continuously decreases (Figure 6). This finding is in line with earlier research on ZnO and doped ZnO NPs' photodegradation of MB. In the absence of catalysts, the breakdown of MB dye was also investigated in the presence of sunshine. As can be observed in Figure 7, in the absence of these catalysts, there was very little MB dye degradation. Additionally, prior findings have shown that a minimum of MB is degraded through photolysis under sunlight.Figure 7. MB dye degradation under sunlight irradiation without using the synthesized NPs.

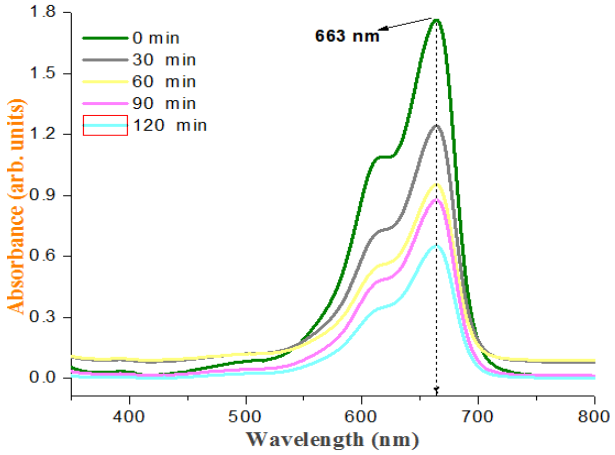

Fig.6. UV absorption spectra of MB using LA doped ZnO NPs.

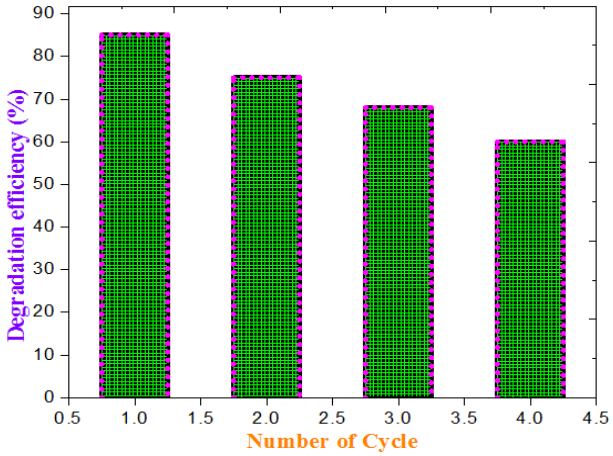

Fig.7. Impact of the LA doped ZnO catalyst dosage on the degradation of the MB dye.

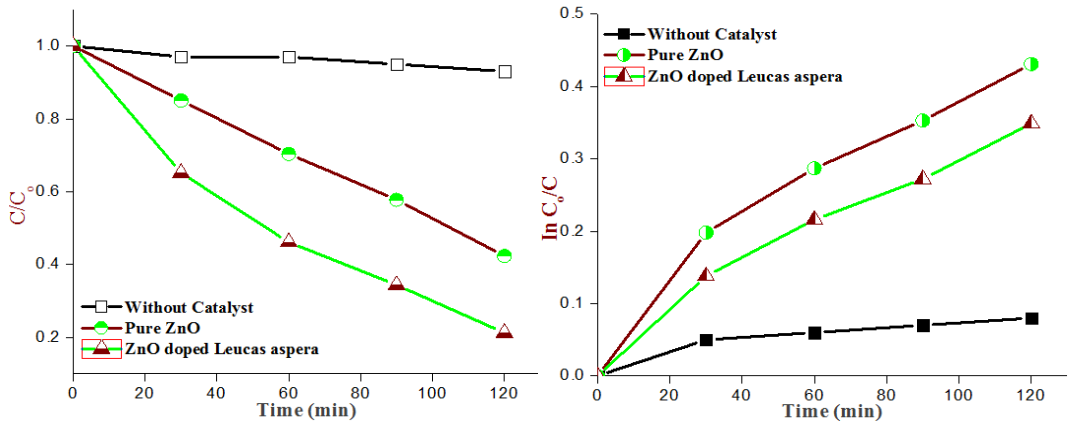

Fig. 8. (a-b) Temporal degradation curve of MB dye using LA doped with ZnO exposed to visible light.

The practical photocatalytic device and waste water treatment uses depend on reproducibility and long-term stability. Under the same experimental circumstances, all catalysts' stability tests were evaluated over five cycles.The relationship is used to compute the absorption percentage of each specific substance. Degradation % = (Co-C)/Cox100 %; where Co is the initial concentration of MB, whereas C is concentration of the dye at various interval times (mole/l), meantime t is the illumination time (min) and k is the reaction rate constant. The experiments are carried out to assess the influence of the catalyst with visible light radiation on the degradation of MB dye and to generate a first-order kinetic constant illustration of C/C_0, as shown in Fig. 8(a-b).The photodegradation efficacy of both dyes has not declined much. After seven cycles of operation, only 2.5 percent of the catalyst's initial degrading effectiveness was lost. Because of this, the catalyst that was gathered is more resilient against the phenol and MB dyes' degradation in the presence of visible light. With time, the photodegradation of MB by doped ZnO NPs under solar radiation increased. The mechanism of ZnO doped LA leaf extract-induced photodegradation of MB is shown in Fig. 9. In fact, water molecules and the highly reactive O_2^* combine to make hydrogen peroxide (H_2O_2), which subsequently reacts with e- in the conduction band to form hydrogen peroxide. This photocatalytic experiment's outcomes showed that doping Mg ions enhanced the ZnO photocatalyst's capacity for photocatalysis.

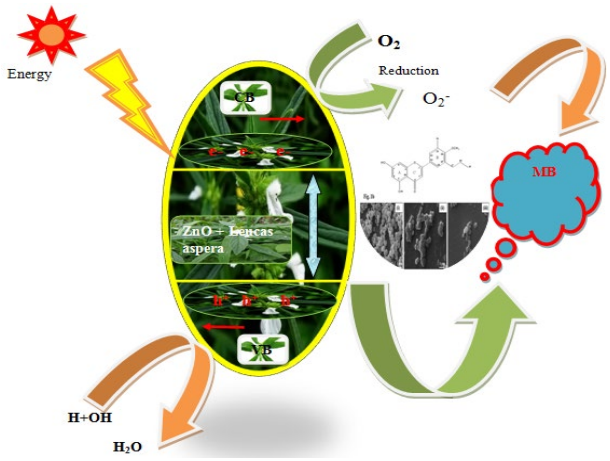

Fig.9.LA doped ZnO catalysts' photocatalytic mechanism when exposed to visible light.

4. Conclusion

Leaf extract from Leucas aspera is an affordable, non-toxic, and environmentally friendly green synthesis method that is effectively used to create both pure and doped ZnO nanoparticles. When compared to pure ZnO nanoparticles, the average particle size derived from the XRD pattern shows that the LA doped ZnO nanoparticles have smaller particle sizes. ZnO doped LA leaf extract nanoparticles' functional groups were detected by FTIR analysis. For the ZnO nanoparticles, it is discovered that the band gap energy is lower. The structure of the synthetic particles is verified by SEM pictures they all seem to be hexagonal wurtzite and somewhat agglomerated. Prepared doped LA-ZnO NPs were found to be crucial to the photocatalytic activity in the study of photodegradation under visible light irradiation. The LA in the ZnO doping acted as an electron scavenger, preventing electron-hole pairs from recombining on the surface of ZnO nanoparticles and thereby enhancing charge transfer.

References

[1] K. Kasinathan, J. Kennedy, M. Elayaperumal, M. Henini, M. Malik, Scientific reports 6 (2016), 1-12; https://doi.org/10.1038/srep38064

[2] S. Logambal, T. Thilagavathi, M. Chandrasekar, C. Inmozhi, Philippe Belle EbandaKedi, F.A. Bassyouni, R. Uthrakumar, Azhaguchamy Muthukumaran, Suresh Naveenkumar, K. Kaviyarasu, J. King Saud Uni. Sci. 35, (2023), 102455; https://doi.org/10.1016/j.jksus.2022.102455

[3] M. Chandrasekar, S. Panimalar, R. Uthrakumar, M. Kumar, M.E. Raja Saravanan, G. Gobi P. Madheswaran, C. Inmozhi, K. Kaviyarasu, Materials Today: Proceedings, 36, (2021), 228-231; https://doi.org/10.1016/j.matpr.2020.03.228

[4] L. Entisar E. Abodi, D.H. Badri Jawad, A. Khafagi. American Journal of Polymer Science, 2(6), (2012); 135-140; https://doi.org/10.5923/j.ajps.20120206.01

[5] R. Vinayagam, G. Sharma, G. Murugesan, S. Pai, D. Gupta, M. Narasimhan, K. Kaviyarasu, T. Varadavenkatesan, R. Selvaraj, J of Mole. Struct., 1263, (2022), 133127; https://doi.org/10.1016/j.molstruc.2022.133127

[6] A. MuhsonNaji, I. Yahiy, M. Safa, H. Mohammed, Mustafa K.A. Mohammed, D.S. Ahmed, Majid S. Jabir, A. Mahdi Rheima, Materials Letters, 322, (2022), 132473; https://doi.org/10.1016/j.matlet.2022.132473

[7] N. Geetha, S. Sivaranjani, A. Ayeshamariam, M. Siva Bharathy, S. Nivetha, K. Kaviyarasu, M. Jayachandran, Journal of Advanced Microscopy Research, 13(1), (2018) 12-19; https://doi.org/10.1166/jamr.2018.1352

[8] S Logambal, M Chandrasekar, R Ashok Kumar, C Inmozhi, S Aravindan, R Uthrakumar, Suresh Naveenkumar, Azhaguchamy Muthukumaran, K Kaviyarasu, J. King Saud Uni. Sci. 36, (2024), 103169; https://doi.org/10.1016/j.jksus.2024.103169

[9] K. Kaviyarasu, X. Fuku, Genene T. Mola, E. Manikandan, J. Kennedy, M. Maaza, Materials Letters, 183, (2016), 351-354; https://doi.org/10.1016/j.matlet.2016.07.143

[10] S. Mangala Nagasundari, K. Muthu, K. Kaviyarasu, Dunia A. Al Farraj, Roua M. Alkufeidy, Surfaces and Interfaces, 23, (2021), 100931; https://doi.org/10.1016/j.surfin.2021.100931

[11] Z. Yuan, J. Li, F. Meng, Journal of Alloys and Compounds, 910, (2022), 164971; https://doi.org/10.1016/j.jallcom.2022.164971

[12] M. Chandrasekar, M. Subash, V. Perumal, S. Panimalar, S. Aravindan, R. Uthrakumar, C. Inmozhi, Abdulgalim B. Isaev, Sudhakar Muniyasamy, A. Raja, K. Kaviyarasu, Separation and Purification Technology, 294, (2022), 121189; https://doi.org/10.1016/j.seppur.2022.121189

[13] C. Maheswari, M. Sathyabama, S. Chandrasekar, G. Gobi, C. Inmozhi, K. Parasuraman, R. Uthrakumar, J. King Saud Uni. Sci. 34, (2022), 102163; https://doi.org/10.1016/j.jksus.2022.102163

[14] K. Raja, P. S. Ramesh, D. Geetha, Structural, Acta Part A: Mole. and Bio. Spect. 131, (2014), 183-188; https://doi.org/10.1016/j.saa.2014.03.047

[15] R. Renuka, K. Renuka Devi, M. Sivakami, T. Thilagavathi, R. Uthrakumar, K. Kaviyarasu, Biocatal. Agric. Biotechnol. 24, (2020), 101567; https://doi.org/10.1016/j.bcab.2020.101567

[16] G. Gomes Miranda, R. Lucasde Sousa Silva, H. Veridiana dos Santos Pessoni, A. Franco Jr, Physica B: Condensed Matter, 606, (2021), 412726; https://doi.org/10.1016/j.physb.2020.412726

[17] S. Panimalar, M. Subash, M. Chandrasekar, R. Uthrakumar, C. Inmozhi, Wedad A. Al-Onazi, Amal M. Al-Mohaimeed, Tse-Wei Chen, J. Kennedy, M. Maaza, K. Kaviyarasu, Chemosphere, 293, (2022), 133646; https://doi.org/10.1016/j.chemosphere.2022.133646

[18] M Subash, M Chandrasekar, S Panimalar, C Inmozhi, K Parasuraman, R Uthrakumar, K Kaviyarasu, Biomass Conv. Bioref. 12, (2022), 1-11; https://doi.org/10.1007/s13399-022-02993-1

[19] V. Perumal, C. Inmozhi, R. Uthrakumar, R. Robert, M. Chandrasekar, S. Beer Mohamed, Shehla Honey, A. Raja, Fahd A. Al-Mekhlafi, K. Kaviyarasu, Environmental Research, 209, (2022), 112821; https://doi.org/10.1016/j.envres.2022.112821

[20] Assumpta C. Nwanya, P.R. Deshmukh, Rose U.Osuji, Malik Maaza, C.D. Lokhande, Fabian I. Ezema, Sensors and Actuators B: Chemical, 206, (2015), 671-678; https://doi.org/10.1016/j.snb.2014.09.111

[21] Abdellah Henni, Abdallah Merrouche, Laid Telli, Amina Karar, Fabian I. Ezema, Hichem Haffar, Journal of Solid State Electrochemistry, 20, (2016), 2135-2142; https://doi.org/10.1007/s10008-016-3190-y

[22] S. Panimalar, R. Uthrakumar, E. Tamil Selvi, P. Gomathy, C. Inmozhi, K. Kaviyarasu, J. Kennedy, Surfaces and Interfaces 20, (2020) 100512; https://doi.org/10.1016/j.surfin.2020.100512

[23] M.D. Tyona, S.B. Jambure, C.D. Lokhande, A.G. Banpurkar, R.U. Osuji, F.I. Ezema, Materials Letters, 220, (2018), 281-284; https://doi.org/10.1016/j.matlet.2018.03.040

[24] I.S. Okeke, K.K. Agwu, A.A. Ubachukwu, M Maaza, F.I. Ezema, Journal of Nanoparticle Research, 22, (2020), 272; https://doi.org/10.1007/s11051-020-04996-3

[25] S. Panimalar, S. Logambal, R. Thambidurai, C. Inmozhi, R. Uthrakumar, Azhaguchamy Muthukumaran, Rabab Ahmed Rasheed, Mansour K. Gatasheh, A. Raja, J. Kennedy, K. Kaviyarasu, Environmental Research, 205, (2022) 112560; https://doi.org/10.1016/j.envres.2021.112560